



# Article

# Development of biodegradable modified starch composite films with *Pleurotus citrinopileatus* polysaccharide and nano titanium dioxide for enhanced fresh-cut yam preservation

Ao Shen<sup>1,†</sup>, Zijun He<sup>1,†</sup>, Jinhong Zhang<sup>1</sup>, Shuzhen Li<sup>2,\*</sup>, and Weiwei Yang<sup>1,\*</sup>

- Department of Food Science, College of Public Health, Shenyang Medical College, Shenyang, China
- <sup>2</sup>Department of Immunology, College of Basic Medical Sciences, Shenyang Medical College, Shenyang, China
- <sup>†</sup>These authors contributed equally to this work.
- \*Correspondence to: Weiwei Yang, Department of Food Science, College of Public Health, Shenyang Medical College, Shenyang 110034, China. E-mail: yangweiwei@symc.edu.cn; Shuzhen Li, Department of Immunology, College of Basic Medical Sciences, Shenyang Medical College, Shenyang 110034, China. E-mail: lishuzhen@symc.edu.cn

#### **Abstract**

Modified starch films are gaining attention as biodegradable and sustainable materials in the food packaging industry. However, their inherent properties, including their brittleness and low antimicrobial and antioxidant capacities, limit their extensive application. To address these shortcomings, in this study, a composite film was developed using potato-modified starch (PMS) as the base material, enhanced with konjac glucomannan (KGM), Pleurotus citrinopileatus polysaccharide (PCP), and nano titanium dioxide (nano TiO<sub>a</sub>). Additionally, PCP and nano TiO<sub>a</sub>, which are bioactive components, were incorporated to improve the functional properties of the films, promoting their application in food preservation. The optimal composition of the composite films was determined through a fuzzy comprehensive evaluation, and the best performance was achieved with 10 g/L of PCP and 1.5 g/L of nano TiO<sub>2</sub>. These composite films exhibited high mechanical strength, antimicrobial capacity, and antioxidant capacity while being noncytotoxic. The practical efficacy of the composite films was verified by applying them to preserve fresh-cut yams at room temperature, where they effectively delayed spoilage and maintained yam quality. This study demonstrates that PMS/KGM/PCP/ nano TiO, composite films can significantly enhance the shelf life of fresh produce, providing a viable route for eco-friendly food preservation.

Keywords: Modified starch films: koniac glucomannan: Pleurotus citrinopileatus polysaccharide: nano titanium dioxide: vam preservation.

### Introduction

Starch is a naturally abundant macromolecular carbohydrate with glucose units linked by glycosidic bonds. Due to its low cost, nontoxicity, and widespread availability, starch has been widely used in food processing applications (Miao and BeMiller, 2023). Specifically, modified starch offers better properties than normal starch. Its biocompatibility and excellent film-forming properties make it suitable for use in developing biodegradable materials, particularly eco-friendly films (Zhang and Zhao, 2017; Su et al., 2023). Despite their advantages, modified starch films have several deficiencies, including high water permeability, poor mechanical strength, low antimicrobial capacity, and low antioxidant capacity (Zhao et al., 2023). These deficiencies limit their practical applications, particularly in food preservation. To improve their mechanical properties and flatness, researchers have explored compounding a polymeric substance, such as gelatin and chitosan, during the preparation of the modified starch films (Soe et al., 2020; Kumar et al., 2021). The introduction of nanoparticles (NPs; commonly ZnO and Ag) is also an innovative and effective solution (Zhang et al., 2022; Qi et al., 2023). The antimicrobial and antioxidant capacities of composite films are critical for the stabilization of wrapped materials, particularly perishable materials, for example, vegetables and fruits. A composite film with high antimicrobial and antioxidant capacities can delay the deterioration of fruits and vegetables due to microbial attack and oxidative reactions. To increase the antimicrobial and antioxidant capacities of modified starch films, bioactive components are commonly introduced. This approach places high demands on the introduced bioactive components, requiring them to offer excellent antioxidant capacity, antimicrobial capacity, and thermal stability.

Based on the above theory, the present study incorporates konjac glucomannan (KGM), Pleurotus citrinopileatus polysaccharide (PCP), and nano titanium dioxide (nano TiO<sub>2</sub>) as functional additives to enhance the properties of modified starch films. KGM, a natural water-soluble heteropolysaccharide, exhibits high water absorption, adhesion, and gelation capability, making it an ideal film-forming agent (Devaraj et al., 2019). PCP, a natural fungal polysaccharide, is known for its diverse biological activities, including

its ability to inhibit microorganisms and oxygen-free radicals (Shen *et al.*, 2023). However, its application in film formation remains relatively unexplored. Nano TiO<sub>2</sub>, recognized for its environmental stability and excellent antimicrobial capacity, can enhance the barrier and mechanical properties of modified starch films when integrated into their matrix (Hoseinnejad *et al.*, 2018). Notably, it remains unknown whether nano TiO<sub>2</sub> can play a corresponding role in the preparation of modified starch films with potato-modified starch (PMS) and KGM to form a film matrix.

During the gelatinization process, the modified starch granules expand significantly while retaining their original structure, leading to the formation of microporous modified starch. This microporous structure facilitates the effective adsorption and encapsulation of bioactive components, preserving their functionality during film preparation (Li *et al.*, 2021).

Yam is a medicinal and edible tuber vegetable that is rich in dietary fiber, vitamins, and minerals. Intact yams generally have a shelf life of more than 2 weeks, which decreases to 3–5 d after mechanical damage. Due to the presence of oxygen and microorganisms, fresh-cut processing can lead to rapid oxidative browning and spoilage of yam within a short period (Ansah *et al.*, 2018; Zhang *et al.*, 2019). Efficient, green, and safe preservation techniques to improve the quality and extend the shelf life of fresh-cut yams are urgently needed.

In this study, we developed a composite film using PMS as the primary substrate, with KGM as a film-forming agent and PCP and nano TiO<sub>2</sub> as supplementary materials. The effects of varying concentrations of PCP and nano TiO<sub>2</sub> on the film's mechanical properties and antioxidant/antimicrobial capacities were thoroughly evaluated. Subsequently, a cytotoxicity test was implemented to evaluate the biosafety of the composite films. Finally, the practical efficacy of the films was verified by evaluating their ability to preserve fresh-cut yams, confirming their potential for application in the food packaging industry.

# **Materials and Methods**

### Materials and reagents

PMS was obtained from Xinrui Biotechnology Co., Ltd. (Suzhou, China). KGM was supplied by Mcklin Biochemical Technology Co., Ltd. (Shanghai, China). PCP with 50% purity was sourced from Shenqing Biochemical Technology Co., Ltd. (Xi'an, China), while nano TiO, was purchased from Jincan Metal Materials Co., Ltd. (Langfang, China). Escherichia coli, Pseudomonas aeruginosa, Staphylococcus albus, Staphylococcus aureus, Aspergillus flavus, and Botrytis cinerea were obtained from the China General Microbiological Culture Collection Center. 293T cells were purchased from the American Type Culture Collection (ATCC). Fetal bovine serum was purchased from Thermo Fisher Scientific (Waltham, MA, USA). Penicillin/streptomycin solution was purchased from Thermo Fisher Scientific (Waltham, MA, USA). Dulbecco's Modified Eagle Medium (DMEM) high-glucose medium was purchased from HyClone (Logan, UT, USA). The CCK8 kit was purchased from Nanjing Jiancheng Bioengineering Institute (Nanjing, China). Fresh yams were acquired from a local farmer's market. All other reagents used in this study were of analytical grade purity (AR) and were procured from standard commercial sources.

# Preparation of PMS/KGM/PCP/nanoTiO<sub>2</sub> composite films

The composite films were prepared using a modified solution-casting method. Initially, 4.5 g of PMS was dispersed in 150 mL of distilled water and heated in a water bath at 100 °C while stirring until a homogeneous paste formed. After the PMS was fully gelatinized, 1.125 g of KGM, varying amounts of PCP (0, 0.75, or 1.5 g), nano TiO $_2$  (0, 0.1125, or 0.225 g), 0.6 g of  $\beta$ -cyclodextrin, and 3 mL of glycerol were sequentially added. Thereafter, the mixture was further stirred in a 70 °C water bath for 10 min to ensure proper dispersion of all the components.

Once the components were thoroughly mixed, the mixture was defoamed by ultrasonication at 70 °C for 15 min and subsequently cooled to room temperature. The film-forming solution was evenly cast onto glass plates (dimension: 30 cm×15 cm) and dried in an oven at 60 °C for 5 h to form the films. After drying, the glass plates of the films were carefully peeled off and incubated at room temperature (20 °C, relative humidity: 35%) for 48 h before further testing.

The groupings and concentrations of PCP and nano  ${\rm TiO_2}$  are shown in Table 1.

# Determination of the composite film properties Thickness

The thickness of the composite films was measured using a CHY-CA thickness gauge (Saicheng Instrument, Jinan, China). Measurements were taken at six randomly selected points on each film, and the average thickness was recorded for further analysis.

## Color difference

The color difference ( $\Delta E$ ) of the composite films was determined using an NR20XE colorimeter (Guangdong Threenh Technology, Guangzhou, China). The  $\Delta E$  value was calculated using the following formula:

$$\Delta E = \sqrt{(L^* - L_0^*)^2 + (a^* - a_0^*)^2 + (b^* - b_0^*)^2}$$
 (1)

 $L^*$ ,  $a^*$ , and  $b^*$  represent the color coordinates of the test sample, and  $L_0^*$ ,  $a_0^*$ , and  $b_0^*$  indicate the reference color coordinates.

### Light transmittance

The composite films were cut into 1 cm×4 cm rectangular pieces, and their light transmittance (T) values at 600 nm were

Table 1. Grouping situation

No.	Group name	Concentration of PCP (g/L)	Concentration of nano TiO <sub>2</sub> (g/L)	
1	0P-0T	0	0	
2	0P-0.75T	0	0.75	
3	0P-1.5T	0	1.5	
4	5P-0T	5	0	
5	5P-0.75T	5	0.75	
6	5P-1.5T	5	1.5	
7	10P-0T	10	0	
8	10P-0.75T	10	0.75	
9	10P-1.5T	10	1.5	

measured using an ultraviolet-visible (UV-Vis) spectrophotometer (Evolution 201, Thermo Fisher Scientific, Waltham, MA, USA). This measurement evaluated the films' optical properties, which are important for their food packaging applications.

## Tensile strength and elongation at break

The mechanical properties of the composite films, including the tensile strength (TS) and elongation at break (E), were measured using a tensile testing machine (C42, MTS, Eden Prairie, MN, USA). The film samples were cut into 1 cm×9 cm strips, and the TS was calculated by applying force until the film fractured. E was recorded as the percentage change in length before the film broke.

#### Moisture content

The composite films were cut into 2 cm×2 cm pieces to determine their moisture content (MC), and their initial weights were recorded as  $m_1$ . Thereafter, the samples were dried in an oven at 105 °C for 24 h, and the final weights were recorded as  $m_2$ . The MC was calculated using the following formula:

$$MC(\%) = \frac{m_1 - m_2}{m_1} \times 100\%$$
 (2)

# Water vapor permeability and CO<sub>2</sub> transmittance

The water vapor permeability (WVP) was measured by sealing a triangular flask containing 5 g of anhydrous CaCl<sub>2</sub> with the composite films. The weight change of the flask was recorded over 24 h, and the WVP was calculated using the following formula:

WVP 
$$\left(\mathbf{g} \cdot \mathbf{mm} / \left(\mathbf{m}^2 \mathbf{d} \cdot \mathbf{kPa}\right)\right) = \frac{\Delta m \times L \times 24}{A \times t \times \Delta P}$$
 (3)

where  $\Delta m$  is the weight change (g), L is the film thickness (mm), A is the surface area of the film (m<sup>2</sup>), t is the time (d), and  $\Delta P$  is the water vapor pressure difference (kPa) between the two sides of the film (Hu *et al.*, 2022).

The CO<sub>2</sub> transmittance was measured by sealing a 50-mL conical flask containing 5 mL of saturated KOH solution with the composite films. The flasks were weighed and stored under ambient conditions for 7 d. The CO<sub>2</sub> transmittance was calculated using the following formula:

$$CO_2$$
 transmittance  $\left( mg / \left( m^2 \cdot h \right) \right) = \frac{\Delta m}{A \times t}$  (4)

where  $\Delta m$  represents the weight difference (mg), A represents the surface area of the film (m<sup>2</sup>), and t represents the duration (h).

### Fuzzy comprehensive evaluation

The optimal composite film was identified through fuzzy comprehensive evaluation (Huang *et al.*, 2020b). Various film properties, including thickness,  $\Delta E$ , T, TS, E, MC, WVP, and CO<sub>2</sub> transmittance, were assigned weights based on their positive or negative effects on the film's overall performance. Specifically, the thickness,  $\Delta E$ , T, MC, WVP, and CO<sub>2</sub> transmittance were considered negative, whereas the TS and E were positive. The assigned weights were as follows: thickness (0.05),  $\Delta E$  (0.05), T (0.15), TS (0.20), E (0.20), MC (0.15), WVP (0.10), and CO<sub>2</sub> transmittance (0.10). The evaluation scores of the composite films were calculated using the following formulas:

For positive attributes:

$$S_{\rm P} = \frac{X_i - X_{\rm min}}{X_{\rm max} - X_{\rm min}} \tag{5}$$

For negative attributes:

$$S_{\rm n} = 1 - \frac{X_i - X_{\rm min}}{X_{\rm max} - X_{\rm min}} \tag{6}$$

Evaluation score = 
$$\sum S \cdot Y_i$$
 (7)

where  $X_i$  represents the actual measured value,  $X_{\min}$  is the minimum measured value,  $X_{\max}$  is the maximum measured value, and  $Y_i$  represents the corresponding weight of each property.

# Antimicrobial capacity

Autoclaved Oxford cups were placed on solid media uniformly coated with 100  $\mu L$  of bacterial or fungal suspension. The following solutions were added to the Oxford cups (200  $\mu L$ ): 0P-0T film solution, 10 g/L PCP solution, 1.5 g/L nano TiO $_2$  solution, 10P-1.5T film solution, saline (negative control), 0.5 g/L streptomycin (positive control for bacteria), and 0.5 g/L fungicidin (positive control for fungi). After the above steps, the four bacterial groups were incubated at 37 °C for 24 h and the two fungal groups were incubated at 30 °C for 48 h. After incubation, the solid media were removed, and the diameters of the inhibition zones were measured in millimeters.

### Antioxidant capacity

The antioxidant capacity of the composite films was evaluated with two radical scavenging assays using 1,1-diphenyl-2-picrylhydrazyl (DPPH) and 2,2'-azino-bis-3-ethylbenzthiazoline-6-sulfonic acid (ABTS\*). To measure the DPPH radical scavenging rate, 5 mL of 0.2 mmol/L DPPH solution was added to centrifuge tubes containing 200 mg of the composite films, which were immersed and shaken for 48 h. The absorbance at 517 nm was measured using anhydrous ethanol as a blank. The DPPH scavenging rate was calculated as follows (8):

DPPH scavenging rate (%) = 
$$\frac{A_0 - A_1}{A_0} \times 100\%$$
 (8)

where  $A_0$  is the absorbance of the DPPH solution and  $A_1$  is the absorbance after interaction with the film.

For the ABTS+ assay, 5 mL of ABTS+ solution was added to centrifuge tubes containing 200 mg of the composite films, which were shaken for 48 h. The absorbance was measured at 734 nm using distilled water as a blank. The ABTS+ scavenging rate was calculated as follows:

ABTS scavenging rate (%) = 
$$\frac{A_2 - A_3}{A_2} \times 100\%$$
 (9

where  $A_2$  is the absorbance of the ABTS<sup>+</sup> solution and  $A_3$  is the absorbance after interaction with the film.

### Chemical structure

The chemical structure of the composite films was analyzed using attenuated total reflection Fourier-transform infrared (ATR-FTIR) spectroscopy (Nicolet iS10, Thermo Fisher Scientific, Waltham, MA, USA). The analysis was performed over a 4000–400 cm<sup>-1</sup> spectral range to detect the

characteristic functional groups and bonding interactions in the film matrix.

## Thermogravimetric analysis

Thermogravimetric analysis (TGA) was conducted to assess the thermal stability of the composite films. The films were heated from 30 to 550 °C under a nitrogen atmosphere at a heating rate of 10 °C/min. The weight loss as a function of temperature was recorded, and the TG curves were analyzed to identify key thermal decomposition events.

### X-ray diffraction

The crystallinity of the composite films was examined by X-ray diffraction (XRD; D8 ADVANCE, Bruker, Bremen, Germany). The measurement was performed at a voltage of 40 kV, current of 40 mA, and 20 scanning range of 10°–80°. The scanning speed was set at 2°/min, following the established protocols for starch-based films (Liu *et al.*, 2023). The diffraction patterns were analyzed to determine the films' crystallinity index and phase structure.

### Microstructure

The surface morphology of the composite films was observed by scanning electron microscopy (SEM) at an accelerating voltage of 5 kV. The films were mounted on stubs and coated with a thin layer of gold before imaging to enhance the surface conductivity. SEM was applied to evaluate the dispersion of the nano  ${\rm TiO}_2$  component and the homogeneity of the film structure.

## Cytotoxicity

The resuscitated 293T cells were cultured in high-glucose DMEM containing 10% fetal bovine serum and 1% penicillin/streptomycin solution. Thereafter, they were incubated at 37 °C in a 5% CO $_2$  incubator. The cells were passaged once every 2 d, and a new medium was introduced once during the period. The cells were inoculated at a density of 2×10 $^4$  cells/well and incubated in 96-well cell culture plates for 24 h. Meanwhile, the DMEM was co-mixed with the following samples at a 3:1 ratio: 0P-0T film solution, 10 g/L PCP solution, 1.5 g/L nano TiO $_2$  solution, and 10P-1.5T film solution. Next, the mixture was incubated for 48 h. The solution and medium in the wells were discarded, and 100  $\mu$ L of a 10% CCK8 solution was added to each well, followed by incubation for 2 h away from light. The optical density at 450 nm was measured.

# Determination of the yam preservation indexes Treatment and storage conditions

Yams were cut into small pieces of approximately 2 cm ×2.5 cm×1.5 cm. The pieces were divided into three groups: a blank group (no treatment), a control group (wrapped with 0P-0T composite films), and a test group (wrapped with 10P-1.5T composite films). The wrapped yam pieces were stored at room temperature (25 °C) and relative humidity of 60% for 8 d. The quality parameters were evaluated at regular intervals (days 0, 2, 4, 6, and 8) at 8 a.m. each day.

## Weight loss rate

The initial weight of the yam pieces (day 0) was recorded as  $m_1$ . Subsequently, the weight of the yam pieces on days 2, 4, 6,

and 8 was recorded as  $m_2$  (Haile, 2018). The weight loss rate was calculated using the following formula:

Weight loss rate (%) = 
$$\frac{m_1 - m_2}{m_1} \times 100\%$$
 (10)

### **Firmness**

The firmness of the yam pieces was measured using a fruit firmness tester (GY-4, Yueqing Aidebao Instrument Co., Ltd., Wenzhou, China) by applying a standard force to determine the resistance to deformation.

### Total soluble solid content

The total soluble solid (TSS) content in the yam pieces was determined by using a handheld refractometer (PAL-1, ATAGO, Tokyo, Japan) to extract juice from the yam samples and subsequently measure the refractive index.

### **Browning**

The browning of the yam pieces was assessed using a colorimeter (NR20XE, Guangdong Threenh Technology, Guangzhou, China). The browning degree was expressed as the  $L^*$  value, which indicates lightness (with high values indicating less intense browning).

### Total phenol content

To analyze the total phenol content, 1 g of yam was ground into a homogenized sample. Ethanol solution (80%) was added at a 1:20 (g/mL) ratio, and the mixture was sonicated for 30 min. The supernatant was collected for analysis after centrifugation at 12 000 r/min for 20 min. A mixture of 1 mL of the diluted extract, 1 mL of Folin-Ciocalteu reagent, and 2 mL of 7% Na<sub>2</sub>CO<sub>3</sub> solution was incubated at 30 °C for 2 h, and the absorbance at 760 nm was measured.

### Polyphenol oxidase activity

The polyphenol oxidase (PPO) activity was determined following the manufacturer's instructions. The PPO activity was exploited to evaluate the enzymatic browning potential of the yam samples.

## Malondialdehyde content

To determine the malondialdehyde (MDA) content, 1 g of yam was homogenized in 5 mL of 100 g/L trichloroacetic acid (TCA) solution in an ice bath. After centrifugation at 12 000 r/min for 20 min, 2 mL of the supernatant was mixed with 2 mL of 0.67% thiobarbituric acid (TBA) solution. The mixture was incubated in a water bath at 100 °C for 20 min and then cooled. Thereafter, absorbance readings were taken at 450, 532, and 600 nm (Hu et al., 2021). The MDA content was calculated using the following formula:

$$MDA \, content \, (\mu \, mol/g) = \frac{c \times V}{V_S \times m} \times 1000 \qquad (11)$$

where c represents the MDA concentration ( $\mu$ mol/L), V represents the total volume of the sample extract (mL),  $V_S$  represents the volume of the sample used for determination (mL), and m represents the sample mass (g).

# Superoxide dismutase activity

The superoxide dismutase (SOD) activity was measured following the manufacturer's protocol. SOD activity is a key indicator of the antioxidant status of yam samples, and it was adopted to evaluate the effectiveness of the composite films in preserving yam quality.

### Statistical analysis

Statistical analysis was performed using SPSS version 27.0 (SPSS Inc., Chicago, IL, USA). One-way analysis of variance (ANOVA) was employed to determine the statistical significance of differences between groups, with *P*<0.05 considered statistically significant. Data visualization and graphs were generated using GraphPad Prism (version 10.0; GraphPad Software, La Jolla, CA, USA).

### Results and discussion

# Determination of the composite film properties Thickness

As shown in Figure 1A, the inclusion of PCP and nano  $\text{TiO}_2$  did not significantly affect the thickness of the composite films.

### Color difference

Without PCP or nano  $\text{TiO}_2$ , the modified starch films exhibited high transparency. The inclusion of PCP imparted a brownish hue to the films, significantly increasing their  $\Delta E$  while maintaining their relative transparency. Conversely, the addition of nano  $\text{TiO}_2$  caused the films to become white and reduced their transparency. As shown in Figure 1B, the maximum  $\Delta E$  was achieved at a nano  $\text{TiO}_2$  concentration of 0.75 g/L. However, as the concentration increased to 1.5 g/L, the  $\Delta E$  decreased. This reduction can be attributed to the balance between the decreased transparency and the neutralization of the PCP's brown color by the increased concentration of nano  $\text{TiO}_2$ . The interplay of these factors caused the  $\Delta E$  to exhibit a decreasing trend as the amount of nano  $\text{TiO}_2$  increased.

### Light transmittance

Films with effective light-blocking properties are beneficial for preserving light-sensitive food products. As shown in Figure 1C, the inclusion of PCP and nano  $\text{TiO}_2$  led to a significant decrease in the T value. Notably, nano  $\text{TiO}_2$  had a greater effect on reducing the T parameter than PCP, indicating that nano  $\text{TiO}_2$  is particularly effective in improving the light-blocking capability of the modified starch films (Goudarzi *et al.*, 2017).

### Tensile strength and elongation at break

The inherent crystalline structure of the modified starch molecules and their intermolecular hydrogen bonding account for their low TS and brittleness (Figures 1D and 1E) (Cui et al., 2021; Mahajan et al., 2021). The integration of PCP into the modified starch matrix created a dense network structure, gradually enhancing the TS of the films. In addition, nano TiO, was uniformly dispersed within the modified starch matrix, enhancing the interfacial interactions and further improving the TS (El-Wakil et al., 2015; Oleyaei et al., 2016). The E was primarily influenced by the concentration of nano TiO<sub>2</sub>, probably due to the dense structure of the films, which limited their flexibility. Although the mechanical properties of the composite films were significantly improved with the inclusion of PCP and nano TiO2, the improvement degree remained lower than that achieved in Zhu's and Poudel's studies (Poudel et al., 2023; Zhu et al., 2023).

### Moisture content

The composite films prepared with PMS and KGM as the film-forming base have a higher MC than those prepared with yam-modified starch or chitosan (Poudel *et al.*, 2023; Shen *et al.*, 2024). As depicted in Figure 1F, the MC of the composite films was significantly influenced by the amount of PCP added. The films with 10 g/L of PCP exhibited a substantially increased MC compared with the films with lower PCP concentrations. This can be attributed to the presence of numerous hydrophilic hydroxyl groups in PCP, which retain moisture within the film matrix (Yousefi *et al.*, 2019). Additionally, the dense film structure likely contributed to the reduced moisture evaporation during drying.

# Water vapor permeability and CO<sub>2</sub> transmittance

Figures 1G and 1H illustrate the effects of PCP and nano TiO<sub>2</sub> on the films' WVP and CO<sub>2</sub> transmittance. The addition of these components increased the hydrophilic hydroxyl content and improved the film density. The dense structure mechanically hindered the transport of water vapor and CO<sub>2</sub>, whereas the hydrophilic groups within the matrix promoted moisture retention (Oleyaei *et al.*, 2016).

#### Fuzzy comprehensive evaluation

The results of the fuzzy comprehensive evaluation reveal that the composite films containing 10 g/L of PCP and 1.5 g/L of nano TiO<sub>2</sub> achieved the best overall performance (Figure 1I). The results indicated that this specific combination of PCP and nano TiO<sub>2</sub> afforded films with optimal properties, particularly in terms of the TS, water vapor barrier, and antioxidant capacity. For further analysis, we focused on two groups: 0P-0T (control) and 10P-1.5T (optimized test group).

#### Antimicrobial capacity

As shown in Table 2, PCP and nano TiO, inhibited all four bacteria and two fungi populations, and the inhibitory effect of PCP on E. coli and Botrytis cinerea even exceeded that of the corresponding positive control. Additionally, in the absence of PCP and nano TiO2, the 0P-0T composite films did not inhibit the growth or reproduction of the microorganisms. In contrast, the ability of the composite films to inhibit microorganisms was significantly improved by the inclusion of PCP and nano TiO<sub>2</sub>. However, the improvement effect was still weaker than that of PCP or nano TiO, alone. This occurs because microorganisms can decompose PMS and KGM into glucose, thereby providing energy for their growth and reproduction. This process weakened the inhibitory effect of PCP and nano TiO, on various microorganisms, making the inhibition zone of the 10P-1.5T composite films smaller than those of the 10 g/L PCP and 1.5 g/L nano TiO<sub>2</sub> groups. In addition, the 10P-1.5T composite films exhibited a greater ability to inhibit microorganisms compared with the cassavamodified starch composite films with 8% ε-PL added (Zhu et al., 2023).

# Antioxidant capacity

Figures 2A and 2B demonstrate that the antioxidant capacity of the composite films was significantly enhanced after the addition of PCP and nano TiO<sub>2</sub>. The DPPH and ABTS radical scavenging assays revealed that films containing these bioactive components exhibited improved free radical scavenging activity, indicating enhanced antioxidant capacity.

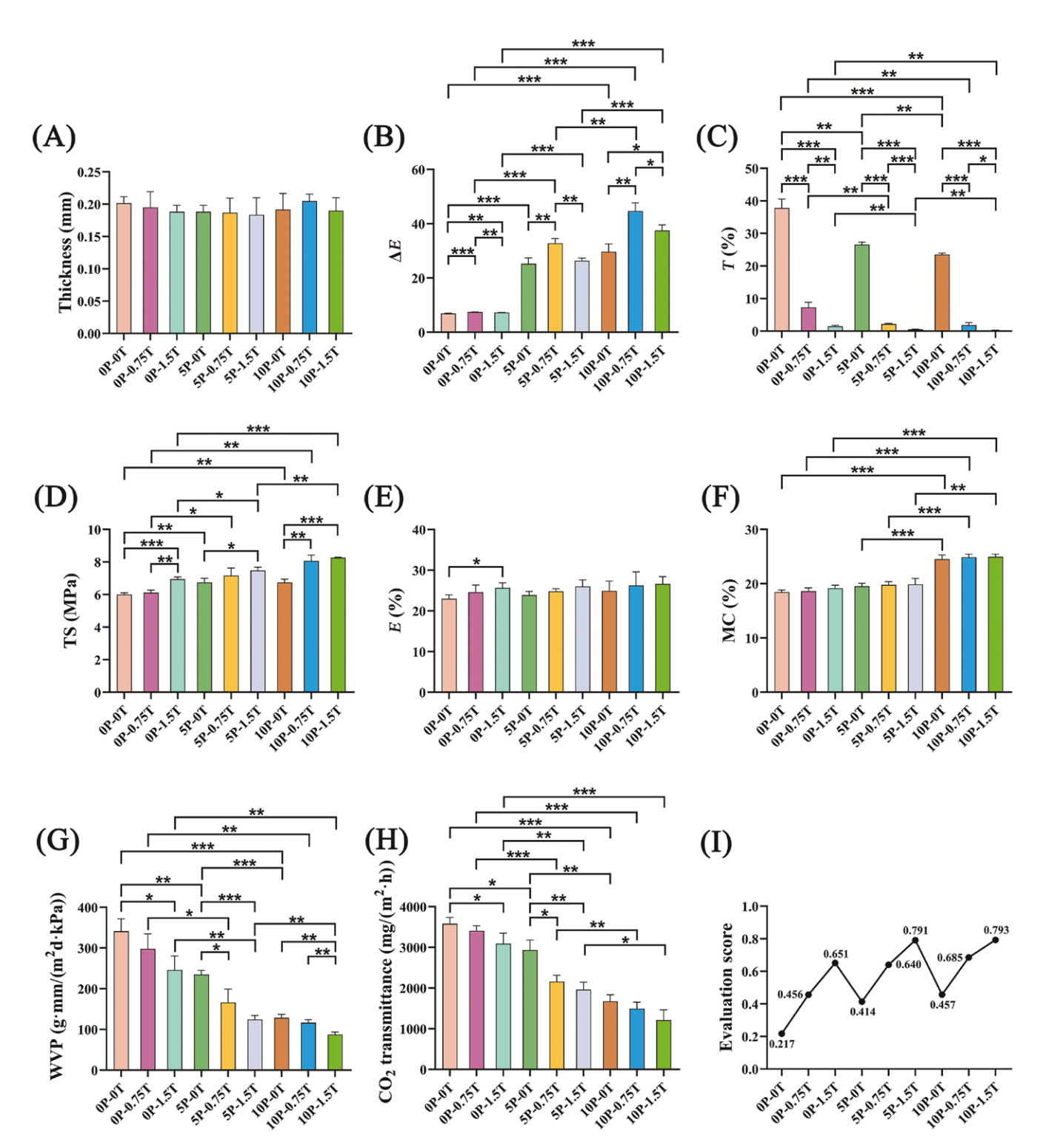


Figure 1. Properties of PMS/KGM/PCP/nano ${\rm TiO}_2$  composite films. (A) Thickness, (B) color difference, (C) light transmittance, (D) tensile strength, (E) elongation at break, (F) moisture content, (G) water vapor permeability, (H)  ${\rm CO}_2$  transmittance, and (I) fuzzy comprehensive evaluation score. \* indicates P < 0.05, \*\* indicates P < 0.01, and \*\*\* indicates P < 0.001.

This improvement can be attributed to the synergistic effects of PCP and nano TiO<sub>2</sub>, which possess inherent antioxidant properties.

### Chemical structure

The Fourier Transform Infrared Spectroscopy (FT-IR) spectra of the two sets of composite films are shown in Figure 2C.

The broad absorption band at 3358 cm<sup>-1</sup> corresponds to the stretching vibration of the hydroxyl (–OH) group, which is indicative of hydrogen bonding among water, glycerol, and the polymer matrix (Tan *et al.*, 2015). The absorption peaks at 2928 cm<sup>-1</sup> and 2864 cm<sup>-1</sup> are attributed to the C–H stretching vibrations within the –CH<sub>2</sub> groups of the modified starch backbone (Seligra *et al.*, 2016). The peak at

Table 2. Name of the strain and diameter of the inhibition zone

No.	Strain	Inhibition zone diameter (mm)						
		0P-0T film solution	10 g/L PCP solution	1.5 g/L nano TiO <sub>2</sub> solution	10P-1.5T film solution	PC	NC	
1	Escherichia coli	_	29.7±2.5*	23.0±1.0*,#	18.3±0.6#	24.0±1.0	_	
2	Pseudomonas aeruginosa	_	17.3±1.5#	15.3±1.5#	15.7±0.6#	35.7±2.1	_	
3	Staphylococcus albus	_	24.7±3.8#	21.7±1.2#	19.7±1.5#	33.7±1.5	_	
4	Staphylococcus aureus	_	31.0±3.0#	27.3±0.6	26.7±2.9#	34.7±2.1	_	
5	Aspergillus flavus	_	21.0±1.0*,#	17.3±3.2*,#	11.7±1.2#	28.0±1.0	_	
6	Botrytis cinerea	_	26.3±2.5*	21.3±1.2*,#	13.3±1.5#	21.3±0.6	-	

<sup>\*</sup>represents a significant difference compared with the 10P-1.5T group, \*represents a significant difference compared with the PC group, and – represents the absence of an inhibition zone.

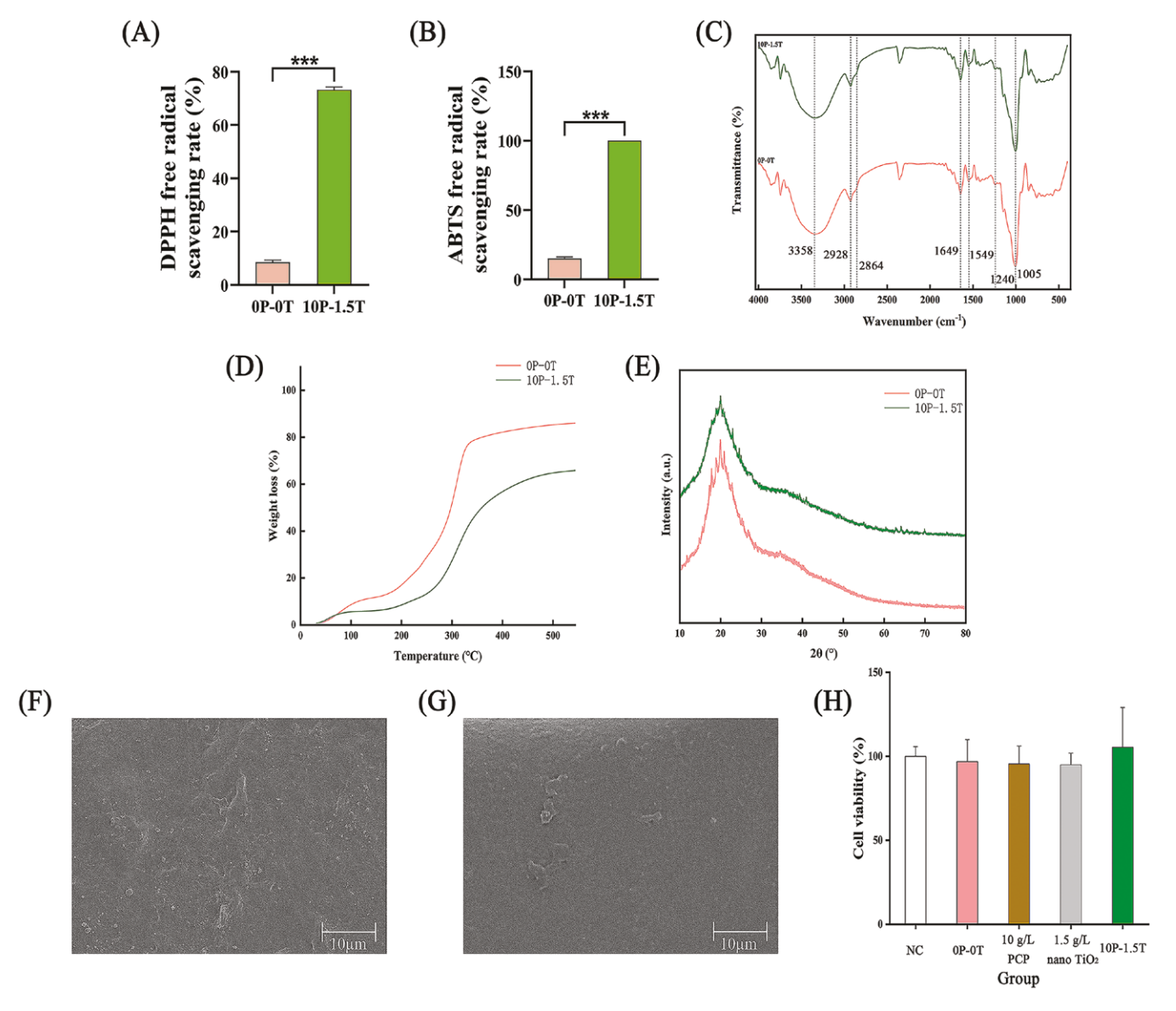


Figure 2. Properties of PMS/KGM/PCP/nanoTiO<sub>2</sub> composite films. (A) DPPH free radical scavenging rate, (B) ABTS free radical scavenging rate, (C) FT-IR spectrogram, (D)TG curve, (E) XRD spectrum, (F) microstructure of the 0P-0T group, (G) microstructure of the 10P-1.5T group, and (H) 48-h cell viability. \*\*\* indicates *P*<0.001.

1649 cm<sup>-1</sup> can be attributed to the bending vibration of the intermolecular hydrogen bonds between the –OH groups in the amorphous region of the modified starch and water

molecules (Phothisarattana *et al.*, 2021). The additional peaks at 1549 cm<sup>-1</sup> and 1240 cm<sup>-1</sup> are assigned to the N–H bending and C–O stretching vibrations, respectively. The

peak at 1005 cm<sup>-1</sup> reflects the C–O stretching in the C–O–C linkages. After incorporating PCP and nano TiO<sub>2</sub>, the FT-IR spectra of the composite films exhibited absorption peaks in the same regions as those of the modified starch films, suggesting that the structural framework of the modified starch matrix remained largely unchanged. This consistency is attributed to the polysaccharide nature of PCP, enabling it to blend well with the modified starch. Additionally, nano TiO<sub>2</sub> did not significantly alter the polymer structure. Zhang *et al.* (2022) reached a conclusion similar to that of the present study, where ZnO was dispersed within the film matrix only in the form of small molecular particles, and no other reactions were involved.

# Thermogravimetric analysis

The TG curves of the composite films, depicted in Figure 2D, reveal two main stages of weight loss. The first stage, occurring between 70 °C and 335 °C, corresponds to the thermal decomposition of PMS, KGM, and PCP, primarily due to the cleavage of glycosidic bonds and the breakdown of hydrogen bonding (Oluwasina et al., 2019). In this stage, the rapid weight loss indicates significant polymer matrix degradation. The second stage, ranging from 335 to 545 °C, is characterized by a slower weight loss or plateau in the TG curve, corresponding to the final dihydroxylation stages. The films containing PCP and nano TiO, exhibited greater thermal stability than those in the control group (0P-0T), as evidenced by the higher residual weight after heating. This enhanced thermal stability can be attributed to the dense structure of the composite films, which requires more energy to undergo depolymerization. This property is also likely due to the reinforcing effects of PCP and nano TiO, (Fu et al., 2018).

### X-ray diffraction

The crystalline structure of the composite films analyzed by XRD is shown in Figure 2E. Both film groups exhibited concentrated diffraction peaks between 17.8° and 22.5°, indicating that the crystalline regions formed from amylose and amylopectin in the modified starch films. These peaks suggest that crystallization is primarily driven by amylose crystallinity and the recrystallization of amylopectin during storage (Li *et al.*, 2020). However, the intensity of these peaks was notably reduced in the spectra of the composite films containing PCP and nano TiO<sub>2</sub>, suggesting that the inclusion of PCP and nano TiO<sub>2</sub> resulted in a decrease in crystallinity (Yousefi *et al.*, 2019).

### Microstructure

The surface morphology of the modified starch films, as observed through SEM, is presented in Figures 2F and 2G. The modified starch films (0P-0T) displayed an uneven surface, characterized by noticeable folds and protrusions, probably caused by the uneven dispersion of the modified starch molecules during film formation. In contrast, the composite films containing PCP and nano TiO<sub>2</sub> presented a smoother surface with fewer visible defects. This phenomenon is consistent with the findings of Yu *et al.* (2011). Despite the improved surface uniformity, some protrusions were still present, probably due to the incomplete dispersion of the additives or residual stresses in the film. Overall, the improved surface morphology of the composite films suggests strong integration of PCP and nano TiO<sub>2</sub> within the modified starch matrix, contributing to the enhanced mechanical and barrier properties.

## Cytotoxicity

As shown in Figure 2H, after 48 h of mixed culture, the 0P-0T film solution, 10 g/L PCP solution, 1.5 g/L nano TiO<sub>2</sub> solution, and 10P-1.5T film solution had no significant effect on the cell viability of the 293T cells. This phenomenon indicated that PCP and nano TiO<sub>2</sub> were not cytotoxic at the current concentration and had sufficient safety.

# Determination of the yam preservation indexes Weight loss rate

The primary factors contributing to the weight loss of vam pieces during storage are moisture evaporation and the consumption of organic matter (Zhang et al., 2019). As illustrated in Figure 3A, the blank group, with no wrapping, exhibited the highest weight loss, reaching 71.28% by the eighth day. A comparison with Zhang et al. (2019) revealed that after 8 d of storage, the fresh-cut yam pieces had an elevated weight loss rate at a temperature of 25 °C and relative humidity of 60%. This significant weight loss can be attributed to the absence of any barrier preventing moisture and gas exchange. In contrast, the weight loss rates of the vam pieces wrapped in the OP-OT and 10P-1.5T films decreased, with the 10P-1.5T group exhibiting the best performance. This superior performance can be attributed to the ability of the composite films to effectively reduce the transmission of water vapor and carbon dioxide, which in turn retarded the respiration and transpiration processes in yam tissues.

#### Firmness

The firmness of the yam pieces decreased over time due to tissue degradation caused by self-respiration, enzymatic activity, and microbial secretion (Figure 3B). The blank group showed the fastest reduction in firmness, reflecting greater tissue breakdown. This trend is similar to that reported in Huang *et al.* (2020a). In contrast, the yam pieces in the 10P-1.5T group retained their firmness significantly longer, suggesting that the PCP and nano TiO<sub>2</sub> in the composite films provided a protective effect. These components likely inhibited the aforementioned destructive factors, thereby preserving the structural integrity of yam tissue.

### Total soluble solid content

The TSS content in the yam pieces, closely related to their nutritional value and flavor, gradually decreased during storage (Figure 3C). This decline was due to the ongoing respiration of the yam pieces, which led to the consumption of organic matter (Li et al., 2018). With no inhibition of respiration, the blank group exhibited the sharpest reduction in the TSS content. Although the TSS contents of the 0P-0T and 10P-1.5T groups were not significantly different, both groups maintained higher TSS levels than the blank group, highlighting the ability of the composite films to preserve the yam's nutritional value. This phenomenon occurs because the composite films hinder gas exchange between the outside and inside parts, thus reducing the consumption of soluble solids via respiration.

## **Browning**

The browning of yam pieces is primarily caused by the enzymatic oxidation of polyphenols, which are converted into brown-colored compounds, such as hydroxyquinone and melanin (Massolo *et al.*, 2011; Chen *et al.*, 2019). Figures 3D and 4 show that the browning degree varied among the

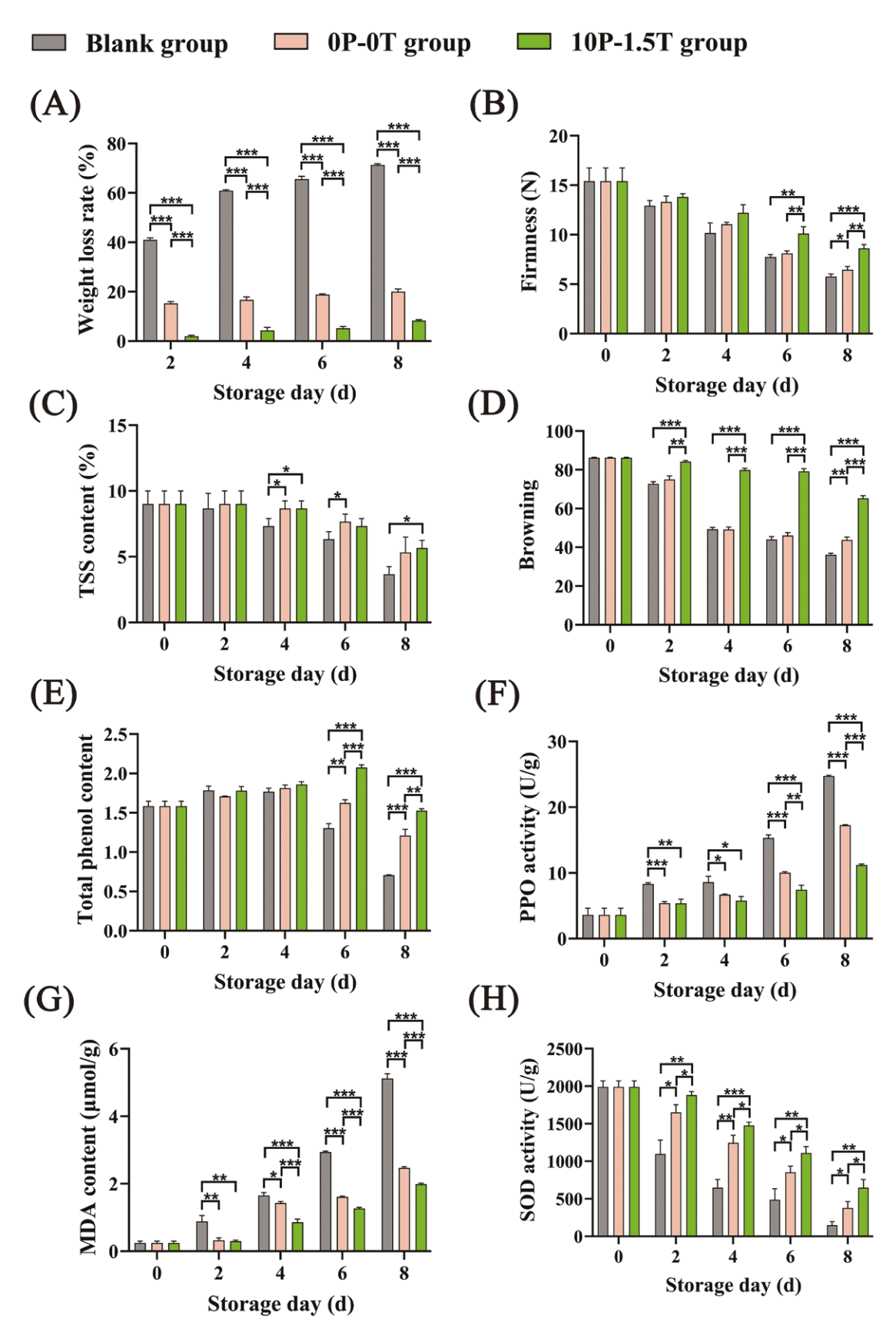


Figure 3. Effects of PMS/KGM/PCP/nano  ${\rm TiO}_2$  composite films on the preservation of fresh-cut yam pieces. (A) Weight loss rate, (B) firmness, (C) TSS content, (D) browning, (E) total phenol content, (F) PPO activity, (G) MDA content, and (H) SOD activity. \*indicates P<0.05, \*indicates P<0.01, and \*indicates P<0.001.

groups. The blank and 0P-0T groups exhibited more pronounced browning as the storage duration increased, whereas the yam pieces in the 10P-1.5T group began to show signs of browning only after the 6th day. This delay in browning can be attributed to the antioxidant and antimicrobial properties of the PCP and nano  ${\rm TiO_2}$  in the composite films, which likely inhibited the PPO activity responsible for browning.

## Total phenol content

As shown in Figure 3E, the total phenol content in the yam pieces initially increased during the early storage period because of the mechanical damage caused by cutting. This induced phenolic synthesis as a defense response in yam tissue. However, as the storage time increased, the total phenol content decreased because of the oxidation and consumption of phenolic compounds. The 10P-1.5T composite films were more effective at preserving the phenol content than the other groups, probably due to their enhanced antioxidant capacity, protecting the phenolics from oxidative degradation.

# Polyphenol oxidase activity

The PPO activity, which catalyzes the oxidation of phenolic compounds and contributes to browning, increased in all the yam samples over the storage period, as illustrated in Figure 3F. The increasing trend of the PPO activity is similar to that reported in Jia's study (Jia *et al.*, 2015). However, the yam pieces wrapped in the 10P-1.5T composite films exhibited significantly lower PPO activity than those in the other groups. This reduction can be attributed to the antioxidant properties of the composite films as well as the ability of the included PCP and nano TiO<sub>2</sub> components to effectively inhibit enzymatic oxidation and delay browning.

### Malondialdehyde content

MDA is a marker of lipid peroxidation, which occurs due to oxidative stress and membrane degradation, particularly under senescent or adverse conditions (Lu *et al.*, 2020). Figure

3G shows that the MDA levels in the blank group increased rapidly throughout the storage period, indicating high levels of oxidative stress and lipid degradation. In contrast, the yam pieces wrapped in the 10P-1.5T composite films exhibited the slowest increase in the MDA content. This suggests that the films provided good protection against lipid peroxidation by limiting oxidative damage, owing to their antioxidant properties.

# Superoxide dismutase activity

SOD is a key antioxidant enzyme that helps protect cells from oxidative stress by catalyzing the dismutation of superoxide radicals (Chiu *et al.*, 2009). As shown in Figure 3H, the blank group displayed the fastest decline in SOD activity due to the high oxidative environment caused by air exposure. In contrast, the 10P-1.5T group maintained relatively high SOD activity throughout the 8-d storage period. This indicates that the composite films effectively preserved the antioxidant status of the yam pieces by reducing oxidative stress, thereby maintaining a high level of enzymatic defense.

## **Conclusions**

We investigated the effects of PCP and nano TiO<sub>2</sub> on the functional properties of modified starch composite films, particularly their performance in preserving fresh-cut yams. The addition of 10 g/L PCP and 1.5 g/L nano TiO<sub>2</sub> significantly improved the mechanical strength, antimicrobial capacity, and antioxidant capacity of the composite films without inducing cytotoxicity. Additionally, the composite films effectively delayed the decrease in quality of the fresh-cut yam samples during storage by reducing moisture loss, browning, and oxidative stress. The findings highlight this novel composite film as a promising material for extending the shelf life of perishable foods, providing a sustainable and biodegradable packaging option for the food industry.

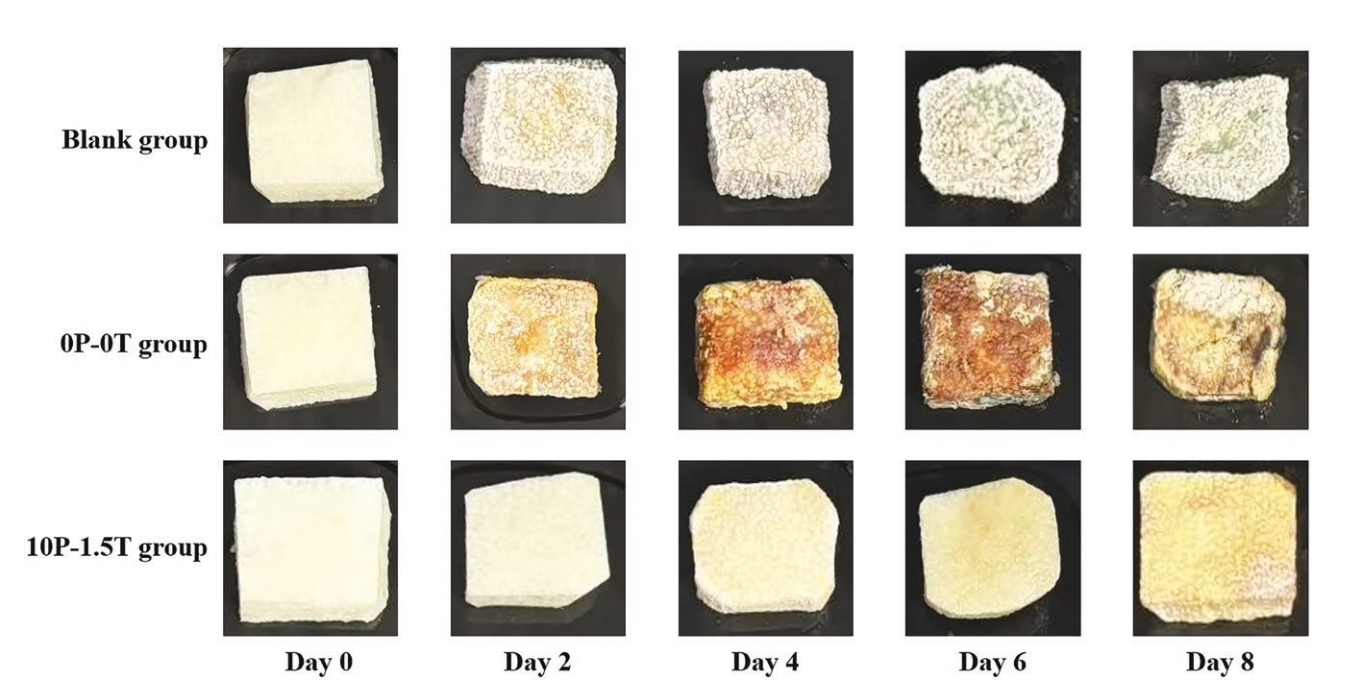


Figure 4. Physical pictures of fresh-cut yam pieces.

# **Author Contributions**

Ao Shen: Conceptualization, data curation, formal analysis, writing original draft, and review and editing; Zijun He: Formal analysis and writing original draft; Jinhong Zhang: Methodology and writing original draft; Shuzhen Li: Project administration, resources, supervision, and review and editing; Weiwei Yang: Funding acquisition, methodology, project administration, supervision, and review and editing.

# **Funding**

This work was supported by the Shenyang Medical College Scientific Research Innovation Fund (Nos. 20182033 and 20191038), China.

# **Conflict of Interest**

The authors declare that they have no conflict of interest related to this article.

## References

- Ansah, F. A., Amodio, M. L., Colelli, G. (2018). Quality of fresh-cut products as affected by harvest and postharvest operations. *Journal of the Science of Food and Agriculture*, 98(10): 3614–3626.
- Chen, B., Wu, G., Li, L., et al. (2019). Effects of 1-methylcyclopropene on the quality attributes of harvested Chinese mushroom (Volvariella volvacea) fruiting bodies. Food Science & Nutrition, 7(2): 747–754.
- Chiu, C. S., Deng, J. S., Hsieh, M. T., et al. (2009). Yam (*Dioscorea pseudojaponica* Yamamoto) ameliorates cognition deficit and attenuates oxidative damage in senescent mice induced by D-galactose. *American Journal of Chinese Medicine*, 37(5): 889–902.
- Cui, Y., Cheng, M., Han, M., et al. (2021). Characterization and release kinetics study of potato starch nanocomposite films containing mesoporous nano-silica incorporated with thyme essential oil. *International Journal of Biological Macromolecules*, 184: 566–573.
- Devaraj, R. D., Reddy, C. K., Xu, B. (2019). Health-promoting effects of konjac glucomannan and its practical applications: a critical review. *International Journal of Biological Macromolecules*, 126: 273–281.
- El-Wakil, N. A., Hassan, E. A., Abou-Zeid, R. E., *et al.* (2015). Development of wheat gluten/nanocellulose/titanium dioxide nanocomposites for active food packaging. *Carbohydrate Polymers*, 124: 337–346.
- Fu, L., Zhu, J., Zhang, S., et al. (2018). Hierarchical structure and thermal behavior of hydrophobic starch-based films with different amylose contents. Carbohydrate Polymers, 181: 528–535.
- Goudarzi, V., Shahabi-Ghahfarrokhi, I., Babaei-Ghazvini, A. (2017). Preparation of ecofriendly UV-protective food packaging material by starch/TiO<sub>2</sub> bio-nanocomposite: characterization. *International Journal of Biological Macromolecules*, 95: 306–313.
- Haile, A. (2018). Shelf life and quality of tomato (*Lycopersicon esculentum Mill.*) fruits as affected by different packaging materials. *African Journal of Food Science*, 12(2): 21–27.
- Hoseinnejad, M., Jafari, S. M., Katouzian, I. (2018). Inorganic and metal nanoparticles and their antimicrobial activity in food packaging applications. *Critical Reviews in Microbiology*, 44(2): 161–181.
- Hu, E. M., Liu, M., Zhou, R., et al. (2021). Relationship between melatonin and abscisic acid in response to salt stress of tomato. Scientia Horticulturae, 285: 110176.
- Hu, D., Zhang, Z., Li, W., et al. (2022). Promoting adsorption performance and mechanical strength in composite porous gel film. *International Journal of Biological Macromolecules*, 223(Part A): 1115–1125.

- Huang, H., Huang, C., Yin, C., *et al.* (2020a). Preparation and characterization of β-cyclodextrin-oregano essential oil microcapsule and its effect on storage behavior of purple yam. *Journal of the Science of Food and Agriculture*, 100(13): 4849–4857.
- Huang, Y., Gu, C., He, S., et al. (2020b). Development and characterization of an edible chitosan-whey protein nano composite film for chestnut (Castanea mollissima Bl.) preservation. Journal of Food Science, 85(7): 2114–2123.
- Jia, G. L., Shi, J. Y., Song, Z. H., et al. (2015). Prevention of enzymatic browning of Chinese yam (*Dioscorea* spp.) using electrolyzed oxidizing water. *Journal of Food Science*, 80(4): C718–C728.
- Kumar, R., Ghoshal, G., Goyal, M. (2021). Biodegradable composite films/coatings of modified corn starch/gelatin for shelf life improvement of cucumber. *Journal of Food Science and Technology*, 58(4): 1227–1237.
- Li, X., Gao, X. X., Lu, J., *et al.* (2018). Complex formation, physicochemical properties of different concentration of palmitic acid yam (*Dioscorea pposita* Thunb.) starch preparation mixtures. *LWT-Food Science and Technology*, 101: 130–137.
- Li, H., Gui, Y., Li, J., et al. (2020). Modification of rice starch using a combination of autoclaving and triple enzyme treatment: structural, physicochemical and digestibility properties. *International Journal of Biological Macromolecules*, 144: 500–508.
- Li, H., Zhai, F., Li, J., et al. (2021). Physicochemical properties and structure of modified potato starch granules and their complex with tea polyphenols. *International Journal of Biological Macro*molecules, 166: 521–528.
- Liu, W., Kang, S., Zhang, Q., et al. (2023). Self-assembly fabrication of chitosan-tannic acid/MXene composite film with excellent antibacterial and antioxidant properties for fruit preservation. Food Chemistry, 410: 135405.
- Lu, C. W., Ding, J. Z., Park, H. K., et al. (2020). High intensity ultrasound as a physical elicitor affects secondary metabolites and anti-oxidant capacity of tomato fruits. Food Control, 113: 107176.
- Mahajan, P., Bera, M. B., Panesar, P. S. (2021). Modification of Kutki millet (*Panicum sumatrense*) starch properties by the addition of amino acids for the preparation of hydrogels and its characterization. *International Journal of Biological Macromolecules*, 191: 9–18.
- Massolo, J. F., Analía, C., Chaves, A. R., et al. (2011). 1-Methylcyclopropene (1-MCP) delays senescence, maintains quality and reduces browning of non-climacteric eggplant (Solanum melongena L.) fruit. Postharvest Biology and Technology, 59(1): 10–15.
- Miao, M., BeMiller, J. N. (2023). Enzymatic approaches for structuring starch to improve functionality. *Annual Review of Food Science and Technology*, 14(1): 271–295.
- Oleyaei, S. A., Zahedi, Y., Ghanbarzadeh, B., et al. (2016). Modification of physicochemical and thermal properties of starch films by incorporation of TiO<sub>2</sub> nanoparticles. *International Journal of Biological Macromolecules*, 89: 256–264.
- Oluwasina, O. O., Olaleye, F. K., Olusegun, S. J., et al. (2019). Influence of oxidized starch on physicomechanical, thermal properties, and atomic force micrographs of cassava starch bioplastic film. *International Journal of Biological Macromolecules*, 135: 282–293.
- Phothisarattana, D., Wongphan, P., Promhuad, K., et al. (2021). Biodegradable poly (butylene adipate-co-terephthalate) and thermoplastic starch-blended TiO<sub>2</sub> nanocomposite blown films as functional active packaging of fresh fruit. Polymers, 13(23): 4192.
- Poudel, R., Dutta, N., Karak, N. (2023). A mechanically robust biodegradable bioplastic of citric acid modified plasticized yam starch with anthocyanin as a fish spoilage auto-detecting smart film. *International Journal of Biological Macromolecules*, 242(Part 2): 125020.
- Qi, Z., Xie, P., Yang, C., et al. (2023). Developing fisetin-AgNPs incorporated in reinforced chitosan/pullulan composite-film and its application of postharvest storage in litchi fruit. Food Chemistry, 407: 135122.

- Seligra, P. G., Medina Jaramillo, C., Famá, L., et al. (2016). Biodegradable and non-retrogradable eco-films based on starch-glycerol with citric acid as crosslinking agent. Carbohydrate Polymers, 138: 66–74.
- Shen, A., Zhang, T. Z., Li, S. Z., et al. (2023). Beneficial effects of Pleurotus citrinopileatus polysaccharide on the quality of cherry tomatoes during storage. Foodborne Pathogens and Disease, 20(9): 398–404.
- Shen, A., Zhang, T. Z., Li, S. Z., et al. (2024). Innovative chitosan-onion polysaccharide composite films: a study on the preservation effects on cherry tomatoes. *Journal of Food Science*, 89(9): 5712–5723.
- Soe, M. T., Pongjanyakul, T., Limpongsa, E., et al. (2020). Modified glutinous rice starch-chitosan composite films for buccal delivery of hydrophilic drug. Carbohydrate Polymers, 245: 116556.
- Su, C. Y., Li, D., Wang, L. J., et al. (2023). Biodegradation behavior and digestive properties of starch-based film for food packaging—a review. Critical Reviews in Food Science and Nutrition, 63(24): 6923–6945.
- Tan, X. Y., Zhang, B. J., Chen, L., et al. (2015). Effect of planetary ball-milling on multi-scale structures and pasting properties of waxy and high-amylose cornstarches. *Innovative Food Science and Emerging Technologies*, 30: 198–207.

- Yousefi, A. R., Savadkoohi, B., Zahedi, Y., et al. (2019). Fabrication and characterization of hybrid sodium montmorillonite/TiO<sub>2</sub> reinforced cross-linked wheat starch-based nanocomposites. *Inter*national Journal of Biological Macromolecules, 131: 253–263.
- Yu, B., Leung, K. M., Guo, Q., et al. (2011). Synthesis of Ag-TiO<sub>2</sub> composite nano thin film for antimicrobial application. Nanotechnology, 22(11): 115603.
- Zhang, S., Zhao, H. (2017). Preparation and properties of zein-rutin composite nanoparticle/corn starch films. Carbohydrate Polymers, 169: 385–392.
- Zhang, G., Gu, L., Lu, Z., et al. (2019). Browning control of fresh-cut Chinese yam by edible coatings enriched with an inclusion complex containing star anise essential oil. RSC Advances, 9(9): 5002–5008.
- Zhang, J., Zhu, L., Li, K. M., et al. (2022). Preparation of bio-based modified starch film and analysis of preservation mechanism for sweet cherry. Food Chemistry: X, 16: 100490.
- Zhao, D., Li, Z., Xia, J., et al. (2023). Research progress of starch as microencapsulated wall material. Carbohydrate Polymers, 318: 121118.
- Zhu, L., Luo, H., Shi, Z. W., et al. (2023). Preparation, characterization, and antibacterial effect of bio-based modified starch films. Food Chemistry: X, 17: 100602.